1950-08

An investigation of capacitor-excited induction generator performance and a verification of a method of performance calculation.

Swift, Charles Shuford

Monterey, California. Naval Postgraduate School

AN INVESTIGATION OF CAPACITOR-EXCITED INDUCTION GENERATOR PERFORMANCE AND A VERIFICATION OF A METHOD OF PERFORMANCE CALCULATION

BY
CHARLES SHUFORD SWIFT

An Investigation Of Capacitor-Excited Induction Generator Performance And A Verification Of A Method Of Performance Calculation

C. S. Swift

AN INVESTIGATION OF CAPACITOR-EXCITED INDUCTION GENERATOR PERFORMANCE AND A VERIFICATION OF A METHOD OF PERFORMANCE CALCULATION

by
Charles Shuford Swift,
Lieutenant, United States Navy.

Submitted in partial fulfillment
of the requirements
for the degree of
MASTER OF SCIENCE
in
Electrical Engineering

United States Naval Postgraduate School
Annapolis, Maryland
1950

This work is accepted as fulfilling
the thesis requirements for the degree of
Master of Science in Electrical Engineering

from the
United States Naval Postgraduate School

Preface

This thesis subject was suggested by Dr. J. B. Friauf of the Navy Department, Bureau of Ships. Dr. Friauf had developed a new method of calculating the performance of a capacitor-excited induction generator, and wished verification of the method by comparison of the calculated performance with the measured performance of an actual generator. It was also hoped that certain unusual performance characteristics shown by calculations could be demonstrated in the actual generator.

An ordinary squirrel cage induction motor was used as the generator. No design data was available on the machine, and the major portion of the project turned out to be the proper determining of the machine constants. Consequently, it is considered worthwhile and pertinent to include in the Appendix the procedure and results in the determination of the machine constants.

It is wished to specifically acknowledge the assistance given by Dr. Friauf, of the Bureau of Ships, and by Professor C. V. C. Terwilliger, of the Postgraduate School, and to thank collectively the members of the Electrical Engineering Department of the Postgraduate School for their individual help and counsel.

This work was performed between August 1949 and June 1950 at the U. S. Naval Postgraduate School, Annapolis, Maryland.

CONTENTS

	Page
Preface	ii
List of Illustrations	iii
Table of Symbols	v
Chapter I Method of Performance Calculation	1
Chapter II Performance Characteristics by Calculation	7
Chapter III Objectives	17
Chapter IV Experimental Procedures	18
Chapter V Results	25
Chapter VI Conclusions	33
Bibliography	34
Appendix	
1. Susceptance Curve	35
2. Blocked Rotor Test	38
3. Division of the Total Resistance Between Primary and Secondary	39
4. Division of the Total Reactance Between Primary and Secondary	41
5. Nameplate Data	44
6. Sample Calculated Data	45

LIST OF ILLUSTRATIONS

Figure	Title	Page
1	Equivalent Circuit For One Phase Of The Shunt Connected Capacitor-Excited Generator	2
2	Equivalent Circuit For One Phase Of The Compound Connected Capacitor-Excited Generator	5
3	Admittance Diagram For Circuit Shown In Figure 1	8
4	Admittance Diagram For Compound Connection	11
5	Admittance Diagram For Circuit Shown In Figure 2	13
6	Experimental Set-Up For The Unity Power Factor Run With Shunt Connected Generator	20
7	Experimental Set-Up For The 0.8 Power Factor Run With Shunt Connected Generator	21
8	Experimental Set-Up For The Unity Power Factor Run With Compound Connected Generator	22
9	Experimental Set-Up For The 0.8 Power Factor Run With Compound Connected Generator	23
10	Shunt Connected Generator-Unity Power Factor Load-External Characteristic	26
11	Shunt Connected Generator-0.8 Power Factor Load-External Characteristic	28
12	Compound Connected Generator-Unity Power Factor Load-External Characteristic	29
13	Compound Connected Generator-0.8 Power Factor Load-External Characteristic	30
14	Susceptance Curve	36
15	Equivalent Circuit For Open Circuit Test	37

Figure	Title	Page
16	Equivalent Circuit For Open Circuit Test With Capacitor Excitation	37
17	Exact Equivalent Circuit For Open Circuit Test With Capacitor Excitation	37
18	Equivalent Circuit For The Short Circuit Test	37
19	Circle Diagram For Determining The Ratio Of R_2/R_1	40
20	Slot and Rotor Dimensions	43

Table of Symbols

r_1	primary resistance per phase to neutral.
r_2	secondary resistance per phase to neutral.
x_1	primary reactance per phase to neutral.
x_2	secondary reactance per phase to neutral.
x_c	reactance of shunt condenser per phase to neutral.
x_3	reactance of series condenser per phase to neutral.
x_m	reactance of magnetizing branch per phase to neutral.
b_m	susceptance of magnetizing branch per phase to neutral.
E_m	voltage across magnetizing branch.
E_T	voltage across shunt condenser.
E_L	voltage across load for compound connected generator.
i_m	current through magnetizing branch.
i_1	primary current.
i_2	secondary current.
s	slip.
ϕ	phase angle.
Y_1	admittance of circuit to the right of points A-B, Figure 1 and 2.
Y_2	admittance of circuit to the left of points A-B, Figure 1 and 2.
Y_m	admittance of magnetizing branch of circuit, Figure 1 and 2.
g	conductance.
b	susceptance.
Z	load impedance.
Z_1	$r_1 + jx_1$.
Z_{1+2}	$R_{1+2} + jX_{1+2}$

R_{1+2}	$r_1 + r_2$.
X_{1+2}	$x_1 + x_2$.
W	watts.
P.F.	power factor.

Chapter I

METHOD OF PERFORMANCE CALCULATION

Because of a renewed interest in the capacitor-excited induction generator by the Navy, Dr. J. B. Friauf, of the Bureau of Ships, developed a new and straightforward method for the calculation of the performance of such a generator. A previous method presented in a paper by C. F. Wagner[5], though satisfactory, involved a laborous, cut-and-try process.

The calculations are based on the following assumptions:

1) That it is sufficient to consider only the fundamental of current and voltage.

2) That the stator and rotor resistance and reactance are constants independent of current and voltage.

3) That the exciting capacitors and the magnetizing branch of the generator equivalent circuit have zero resistance.

4) That the frequency of the generator output is kept constant, the speed of the generator being regulated as necessary to satisfy this condition.

The equivalent circuit for one phase of the generator is shown in Figure 1 with the notation used. From Kirchhoff's Laws, the currents at point B sum to zero.

$$i_m + i_1 + i_2 = 0 \qquad (1)$$

If E_m is the voltage between A-B, then $i_1 = E_m Y_1$, $i_2 = E_m Y_2$, and $i_m = E_m Y_m$. Substituting in Equation (1), when E_m is not

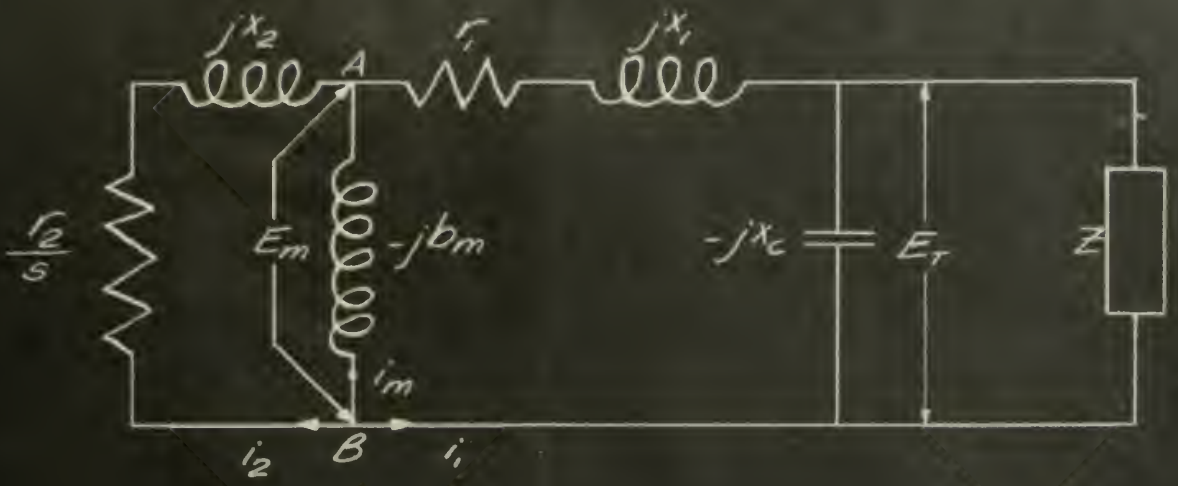

$r_1 = 0.440$ ohms $\quad X_1 = 0.810$ ohms

$r_2 = 0.327$ ohms $\quad X_2 = 0.584$ ohms

$X_c = 15.48$ ohms

EQUIVALENT CIRCUIT FOR ONE PHASE OF THE SHUNT CONNECTED CAPACITOR-EXCITED INDUCTION GENERATOR

FIGURE 1

equal to zero, gives:

$$Y_m + Y_1 + Y_2 = 0 \qquad (2)$$

This is the fundamental equation upon which Dr. Friauf's method of calculation is based.

Each of these admittances depends on only one variable if the exciting capacitance and the power factor of the load are kept constant.

Y_1 varies with the load impedance. It may be calculated from:

$$Y_1 = \frac{1}{r_1 + jx_1 + \dfrac{1}{\dfrac{1}{-jx_c} + \dfrac{1}{|Z|(\cos \phi + j \sin \phi)}}} \qquad (3)$$

or from its locus, which is a circle with center and radius as defined as follows:

$$x = \frac{r_1 + \frac{1}{2}x_c \tan \phi}{r_1^2 + x_1^2 + x_c(r_1 \tan \phi - x_1)} \qquad (4)$$

$$y = \frac{\frac{1}{2}x_c - x_1}{r_1^2 + x_1^2 + x_c(r_1 \tan \phi - x_1)} \qquad (5)$$

$$R = \frac{\frac{1}{2}x_c \sec \phi}{r_1^2 + x_1^2 + x_c(r_1 \tan \phi - x_1)} \qquad (6)$$

Y_2 varies only with the slip, and may be calculated from:

$$Y_2 = \frac{\frac{r_2}{s} - jx_2}{\frac{r_2^2}{s^2} + x_2^2} \qquad (7)$$

Y_m varies with the voltage between A and B, and is found from Equation (2).

$$Y_m = -Y_2 - Y_1 \qquad (8)$$

With Y_m the Susceptance Curve is entered and the value of E_m, the voltage between A and B, is picked off. The determination of this curve is given in the Appendix. The current through the load and the voltage across the load are found by use of Equations (9), (10) and (11).

$$E_m Y_1 = i_1 \qquad (9)$$

$$E_T = E_m - i_1 Z_1 \qquad (10)$$

$$i_L = i_1 - E_T/-jx_c \qquad (11)$$

A complete and detailed explanation of the method may be found in Dr. Friauf's paper [2].

The procedure is the same for the compounded generator, the equivalent circuit for one phase being shown in Figure 2.

Y_1 may be calculated from:

$$Y_1 = \frac{1}{r_1 + jx_1 + \frac{1}{\frac{1}{-jx_c} + \frac{1}{Z(\cos\phi + j\sin\phi) - jx_3}}} \qquad (12)$$

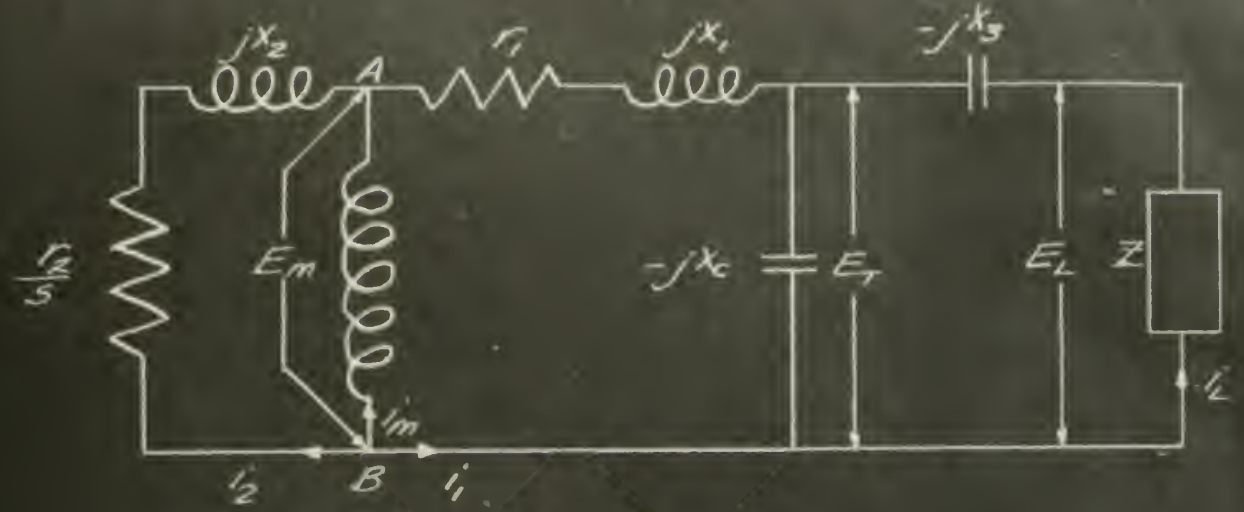

r_1 = 0.440 ohms X_1 = 0.810 ohms

r_2 = 0.327 ohms X_2 = 0.584 ohms

X_c = 20.1 ohms X_3 = 15.0 ohms

EQUIVALENT CIRCUIT FOR ONE PHASE OF THE COMPOUND CONNECTED CADACITOR-EXCITED INDUCTION GENERATOR

FIGURE 2

or found from its locus, which is a circle with center and radius defined as follows:

$$x = \frac{r_1 + \frac{1}{2}x_c \frac{x_c}{x_c+x_3} \tan \phi}{(r_1+\frac{1}{2}x_c \frac{x_c}{x_c+x_3}\tan \phi)^2 + (x_1-\frac{1}{2}x_c\frac{x_c+2x_3}{x_c+x_3})^2-(\frac{1}{2}x_c \frac{x_c \sec \phi}{x_c+x_3})^2} \quad (13)$$

$$y = - \frac{x_1 - \frac{1}{2}x_c \frac{x_c + 2x_3}{x_c + x_3}}{(\text{same denominator as (13)})} \quad (14)$$

$$R = \frac{\frac{1}{2}x_c \frac{x_c}{x_c + x_3}\sec \phi}{(\text{same denominator as (13)})} \quad (15)$$

Y_2 is of course the same for both the shunt and compounded generators.

$Y_m = -Y_2 - Y_1$, as before, and is used as in the shunt case to find E_m. The current through the load and the voltage across the load are found by using Equations (9), (10), (11) and (16).

$$E_L = E_T - i_L(-jx_3) \quad (16)$$

This method is not without labor, however, it is straightforward, and by using a tabular form similar to the sample calculations shown in the Appendix the work is not difficult.

Chapter II

PERFORMANCE CHARACTERISTICS BY CALCULATION

The variation of the voltage across the load and the current through the load with load changes will be called, in this paper, the external characteristics of the generator. The capacitors will be considered part of the generator system, rather than the load. This is purely arbitrary.

The performance characteristics of the capacitor-excited induction generator may be readily predicted and analyzed by the use of the admittance diagram for the equivalent circuit. For the circuit with the capacitors shunted across the load, Figure 1, the admittance diagram is as shown in Figure 3.

In Figure 3 the curves labeled Y_1 and $-Y_2$ are the locii of the vectors representing the admittances Y_1 and $-Y_2$. These locii are circles. A proof of this is given in Dr. Friauf's paper. Each point on Y_1 corresponds to a specific load, and each point on $-Y_2$ corresponds to a specific slip. Since Y_m is assumed to be a pure susceptance it will be a vector directed vertically downward.

It can be seen from the admittance diagram that for a given load the generator must operate at the slip on the $-Y_2$ locus directly below this load on the Y_1 locus in order that the Y_m vector be vertical and have a magnitude equal to the vectorial difference between $-Y_2$ and Y_1.

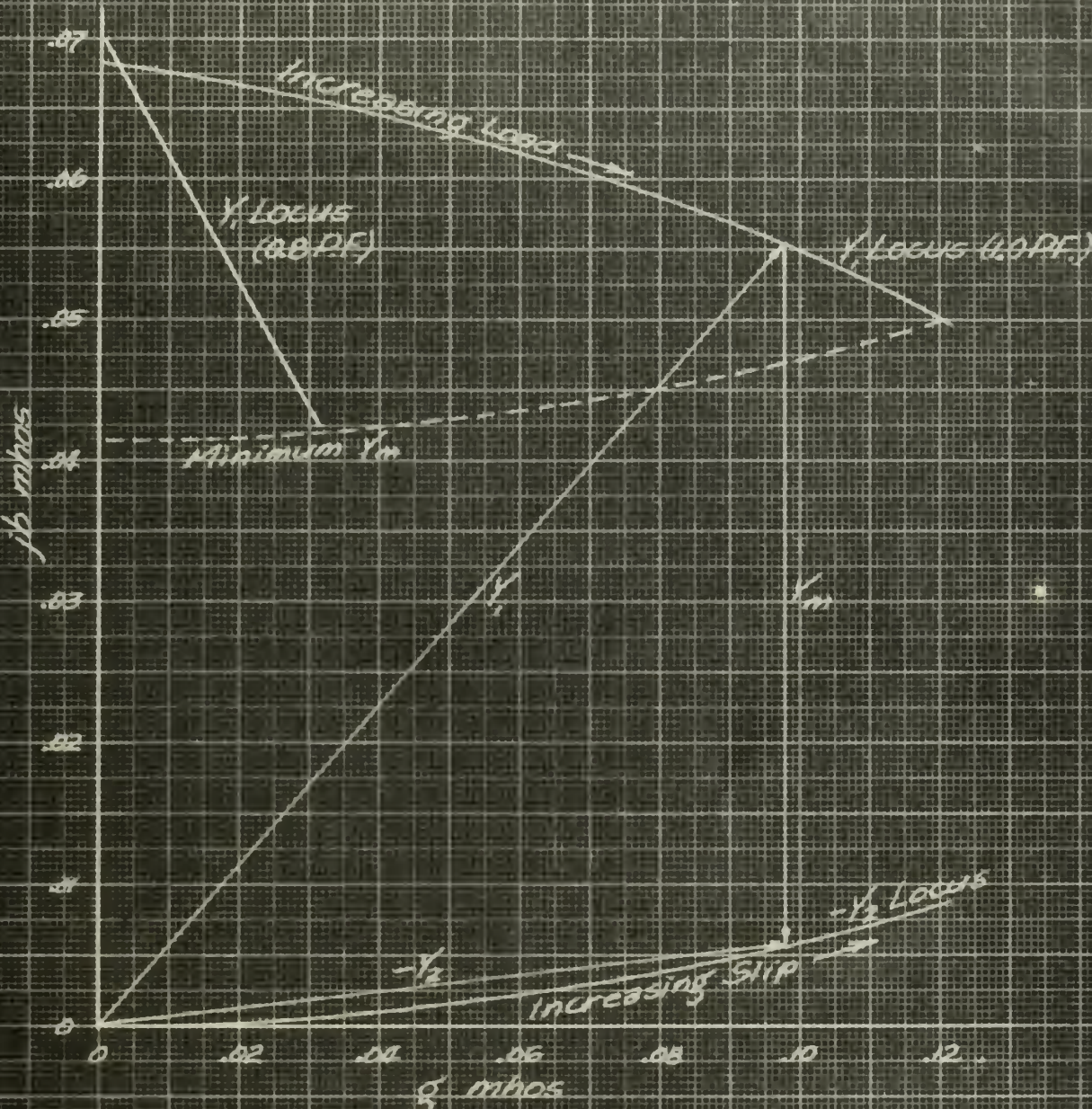

ADMITTANCE DIAGRAM FOR CIRCUIT SHOWN IN FIGURE 1

FIGURE 3

As the load is increased the difference, $-Y_2-Y_1 = Y_m$, decreases until a minimum value of Y_m is reached at which the machine will no longer operate as a generator. This minimum value of Y_m is shown on Figure 3. It corresponds to the straight portion of the magnetizing curve for the machine, or the vertical portion on the susceptance curve, Figure 14.

Physically in the generator, the load increase, or load impedance decrease, reduces the voltage across the shunt capacitor until it will no longer cause enough current to flow through the capacitor to excite the generator.

The shapes of the locii show that the shunt capacitor-excited induction generator will have a drooping characteristic for unity power factor and lagging loads, and that this droop will be very pronounced as the power factor decreases. Further, as the load impedance decreases and the shunt capacitor is shorted out the generator will cease to generate, as previously pointed out, thus the shunt connected, capacitor-excited, induction generator cannot deliver a short circuit current to a unity power factor or lagging load. The resultant external characteristics are shown in Figures 10 and 11.

The admittance diagram also points out that in designing an induction generator the magnetizing circuit should saturate as rapidly as possible, the rotor resistance should be high, and the rotor reactance low.

By varying the values of x_c in Equations (4), (5) and (6) within reasonable limits it is seen that an increase in

shunt capacitance will increase the radius of the Y_1 circle, and raise it. Only the unity power factor case was considered, but the results would be qualitatively the same for the lagging cases. Reasonable limits for the increase of capacitance for the generator used in the test were considered to be from 135 microfarads, the minumum required for excitation, to 500 microfarads. A higher, flatter Y_1 curve results in a higher no-load voltage, better regulation, and a greater load carrying capacity. The increased capacitance causes operation higher on the magnetizing and susceptance curves.

However, an examination of the equivalent circuit shows that this increase in capacitance effects an increase in exciting current as well as an increase in load current. Since it is the sum of these two currents that passes through the generator, it might well be overloaded before appreciable load current is being delivered. In the extreme, it might be overloaded internally while delivering no external load. Strictly speaking the shunt capacitors are also a load.

For the compounded circuit, Figure 2, with capacitors in series with the load, as well as the shunt capacitors, the $-Y_2$ and Y_m locii on the admittance diagram are the same as in the shunt case, of course, however, the Y_1 locii are as shown in Figure 4.

An examination of these locii shows that, in contrast to the shunt connected generator, the compound connected generator will always deliver a short circuit current. Calculations

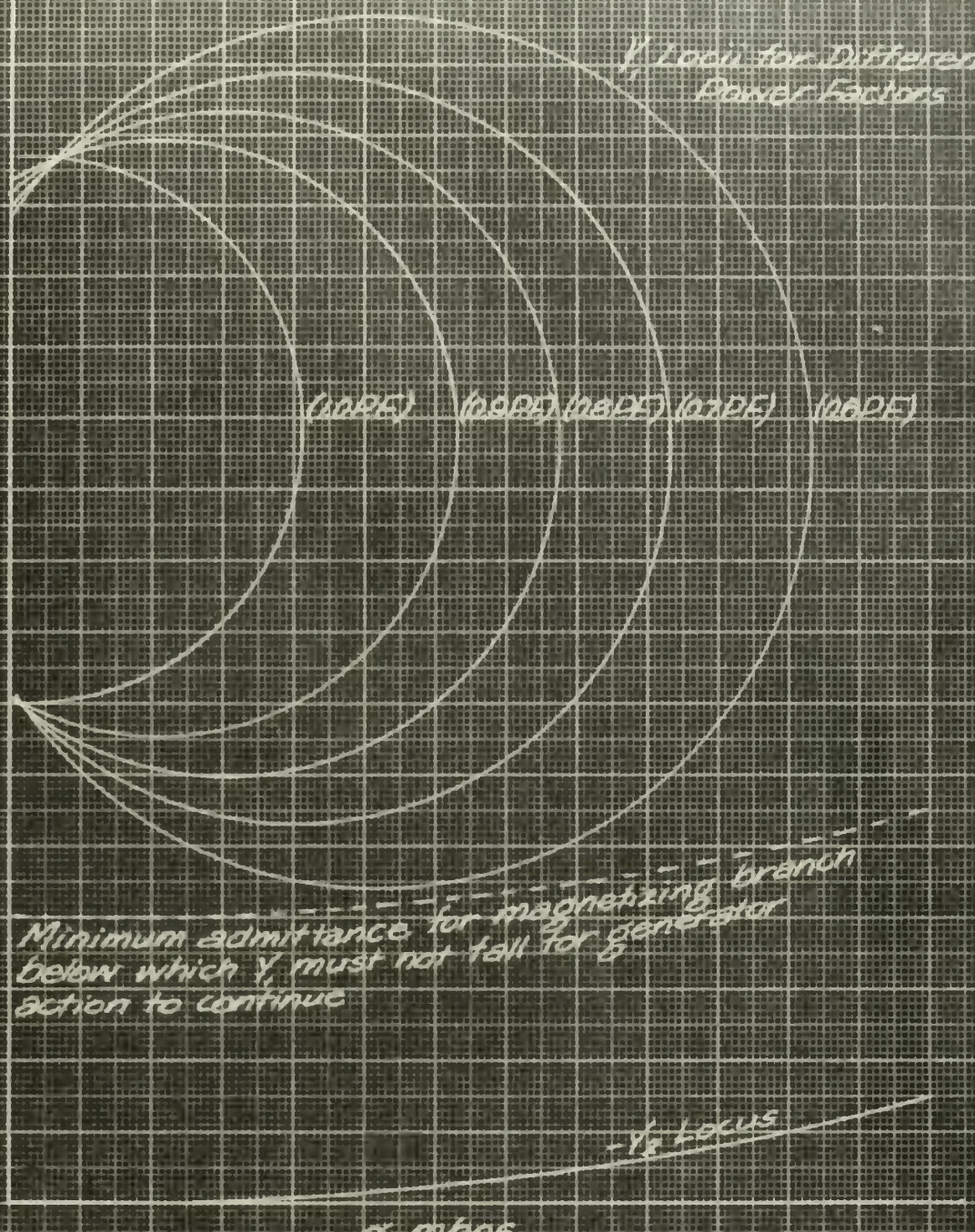

ADMITTANCE DIAGRAM FOR COMPOUNDED CONNECTION

FIGURE 4

reveal that the external voltage first falls as the load increases, then rises, and finally falls to zero as short circuit is approached. The reason for the initial droop and following rise can be seen in the shapes of the Y_1 locii. As the load is increased the voltage across the shunt capacitor is reduced and less exciting current flows through it. Current flow increases through the series capacitor. At first the current through the series capacitor does not compensate for the loss of exciting current through the shunt capacitor, but as the load is further increased the series capacitor becomes more and more effective, until the current through it does compensate for the loss of exciting current through the shunt capacitor. As the load continues to increase the excitation finally becomes greater than the no-load excitation and the result is a rise in the external voltage above the no-load voltage. On short circuit the series capacitance is in effect added to the shunt capacitor.

The admittance diagram shows that for certain choices of shunt and series capacitance it would be possible to maintain exciting current, and thus load, for all reasonable power factors. (See Figure 4). In Figure 5 is shown a case in which for power factors below 0.8, load will be lost for a while and then regained. It would be impossible to operate at some certain power factors and loads.

Physically, this corresponds to the condition described previously, where the load impedance has been reduced until

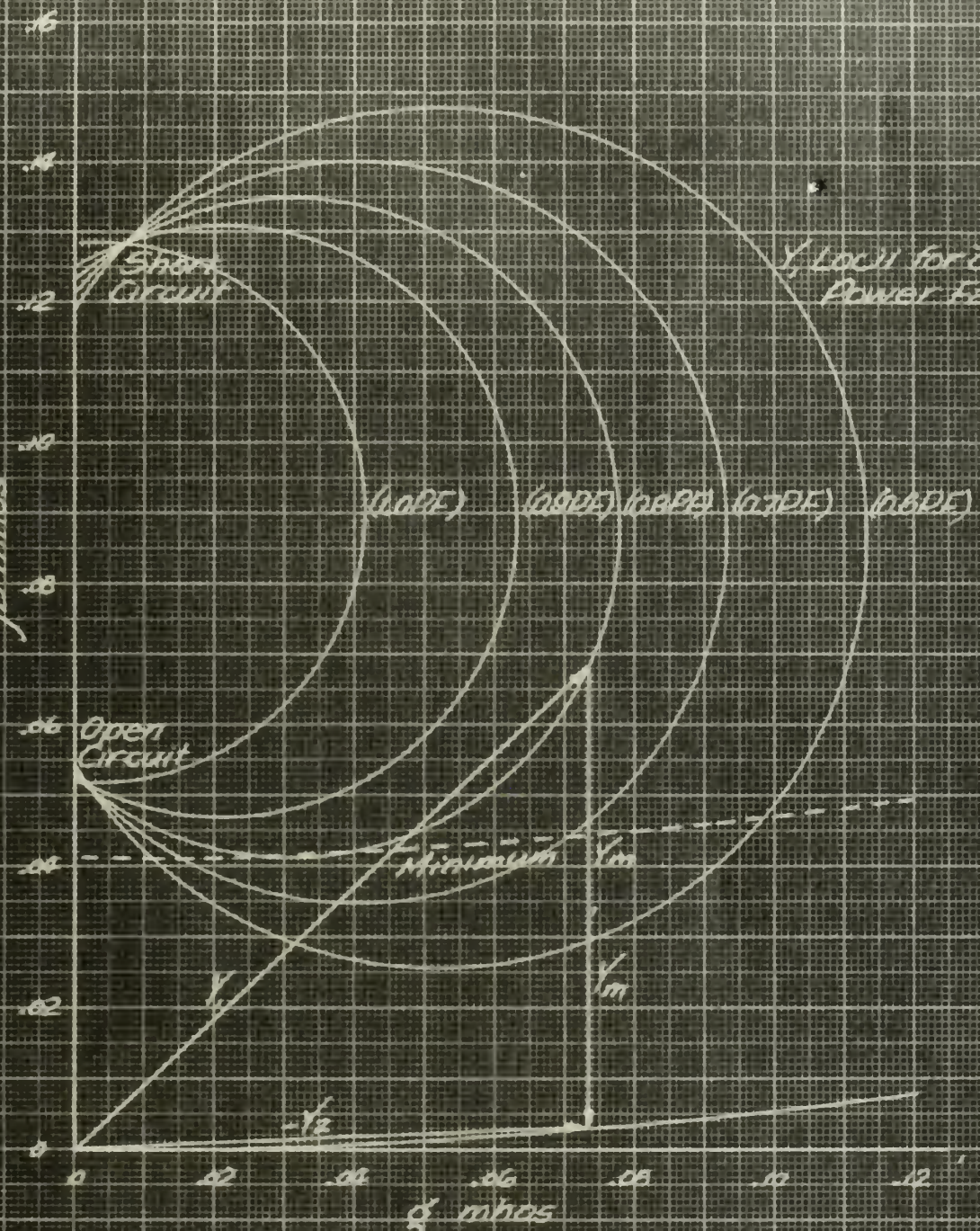

ADMITTANCE DIAGRAM FOR CIRCUIT SHOWN IN FIGURE 2

FIGURE 5

the voltage across the shunt capacitor no longer caused enough exciting current to flow through it. The current through the series capacitor does not compensate enough for this loss, and the loss of exciting current falls to a value which will no longer support generator action. When the load impedance has been further reduced to allow more current through the series capacitor, enough exciting current will flow, and generator action will commence again.

Another interesting aspect of the compounded generator is that the slip will increase to a maximum value, and then decrease to nearly zero at short circuit. This is logical since the slip is a measure of the torque, and therefore the power being delivered, and the power delivered to the load is zero at no load, rises to a maximum, and then drops to zero again at short circuit, where the voltage across the load is zero.

It will be noted in the sample calculations that at zero slip the load current is negative. This merely means that at zero slip the generator will not generate because there will be no currents in the secondary or rotor. Consequently, it cannot excite itself, and the exciting current must be supplied from the load.

By varying the values of x_c and x_3 in Equations (13), (14) and (15), and using the constants of the test generator, the changes in generator performance may be easily predicted both quantitatively and qualitatively for these variations.

The same reasonable limits of variation are used for x_c and x_3 as in the previous shunt case. Holding x_3 constant at 15 ohms and increasing the shunt capacitor raises the Y_1 circle and increases the radius as in the shunt case. The circle rises rapidly (from 0.05 to 0.20 mhos), but the increase in the radius is slight (from 0.038 to 0.47 mhos). Holding x_c constant at 20 ohms and increasing the series capacitance results in a rapid increase in the radius of the Y_1 circle (from 0.038 to 0.131 mhos) and very little raising of the circle (from 0.052 to 0.053 mhos). In both cases the center of the circle moves so slightly to the right as to produce little effect on the performance, and is, therefore, neglected.

Decreasing x_c helps reduce the initial droop, however, as in the shunt generator, but in an even more pronounced way, it increases the generator internal load in greater proportion than the external load carrying capacity. Decreasing x_3 increases the load carrying capacity more nearly in proportion to the increase in the total internal load. Thus decreasing x_3 gives a greater gain than a decrease in x_c. If x_3 is made too small the generator may destroy itself on short circuit, because of the tremendous exciting current that will flow. X_c should be the maximum value that will give a reasonably flat external characteristic curve, that is a reasonable amount of initial droop. X_3 should be the minimum value possible without endangering the machine on

short circuit or heavy loads.

Calculated external characteristics for the compounded generator used are shown in Figure 12 and 13.

Chapter III

OBJECTIVES

The primary objective of the thesis is to verify the method of capacitor-excited induction generator performance calculation developed by Dr. Friauf. The verification is to be by comparing calculated external characteristic curves with the measured external characteristics of an actual generator, for both the shunt connection and the compound connection, and for lagging as well as unity power factors.

The second objective is to verify the performance characteristics shown by the calculations by demonstrating them in the actual generator. Specifically, it is hoped to produce the characteristic shown by calculations for the compounded generator for certain lagging power factor loads where excitation is lost for a certain range of loads, and then regained. This is the condition described in Chapter II where the Y_1 circle drops temporarily below the minimum line for excitation (Figure 5).

No investigation is desired at leading power factors, because the generator is always excited at these power factors and, within limits, will always deliver power.

Chapter IV

EXPERIMENTAL PROCEDURE

A Westinghouse 5 KVA, 220 volt, squirrel cage induction motor was used as the induction generator. It was driven by a DC motor in order to get the variable speed required to keep the frequency constant. The motor nameplate data is given in the Appendix.

The revolutions per minute of the generator were measured at each load by a revolution counter which counted the revolutions for a period of ten seconds, and was marked to read revolutions per minute directly.

In all of the tests phase values of current, voltage and watts were measured. The instrument wiring is shown in the wiring diagrams for each set-up. It was impossible to put instruments in each phase, which required that the instruments be shifted from phase to phase. Every effort was made to insure that the load was balanced.

The frequency was measured by an electronic frequency meter, and the speed of the DC drive varied to maintain the frequency constant at 60 cycles. An accuracy of $\pm 2\%$ was claimed for the frequency meter.

The capacitors were measured on an impedance bridge. In all set-ups the phases were balanced to within 0.5 microfarads.

For the unity power factor run with the shunt generator the wiring diagram, Figure 6, shows the set-up used.

Two loads were used, a wound resistor bank, and a lamp bank.

For the 0.8 power factor run with the shunt generator the wiring diagram, Figure 7, shows the set-up used. A synchronous motor driving a DC generator which loaded a resistor bank was used as the load. The power factor was measured by a single phase power factor meter, and was kept at 0.8 by varying the excitation of the synchronous motor. This system worked very well.

For the compounded generator lamp banks were again used for the unity power factor load, and the set-up is shown in Figure 8.

For the 0.8 power factor run with the compounded generator the synchronous motor and DC generator set-up was tried, but found to be impractical. It could not be made to provide the load and power factor required. The system could not be stabilized. A static load was used with variable inductance in series with variable resistance. The inductance was varied by changing the amount of iron in the core of the inductance, and by varying the connections of the inductances from series to shunt. The load was connected in Y in order to have a neutral for phase measurements. The set-up is shown in Figure 9.

Two runs were made with each load for the shunt generator. The press of time allowed only one run for each load for the compounded generator.

The value of capacitance chosen for the shunt generator was selected to give the generator as high a load carrying

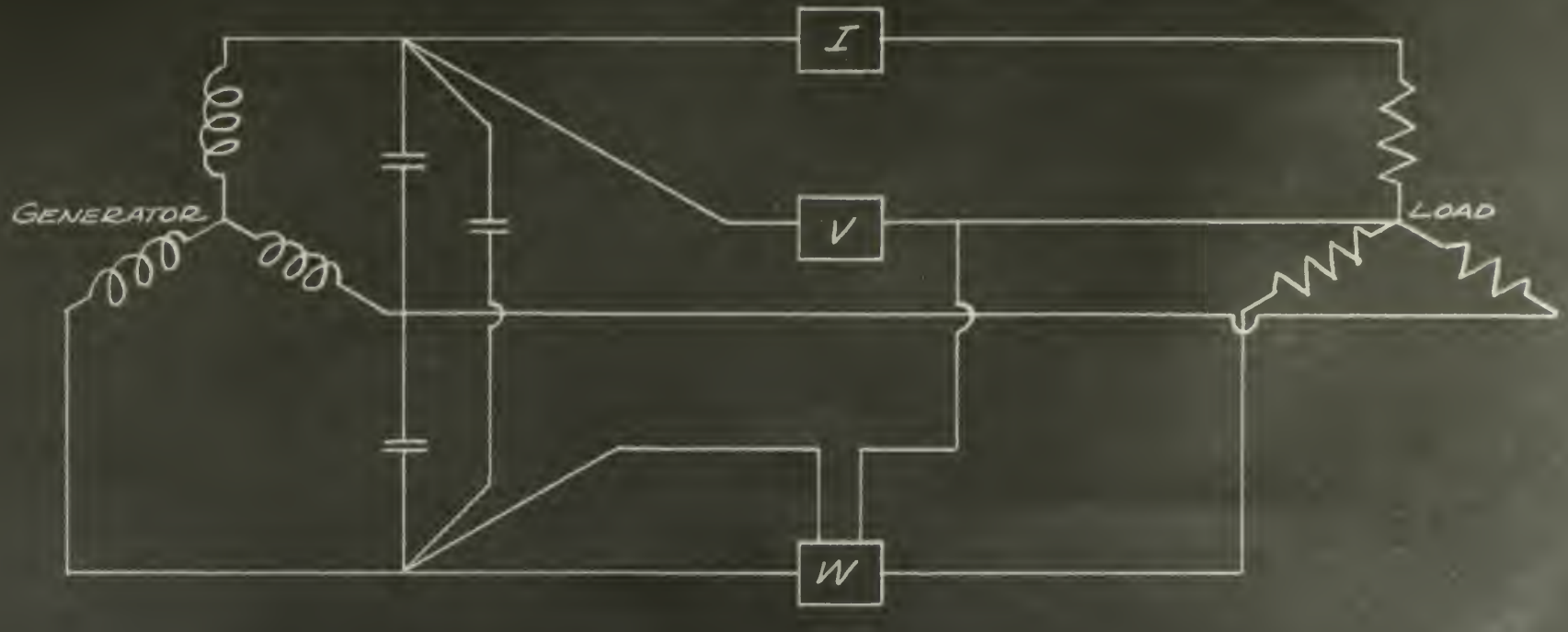

FIGURE 6

EXPERIMENTAL SET-UP FOR THE UNITY POWER FACTOR RUN WITH SHUNT CONNECTED GENERATOR

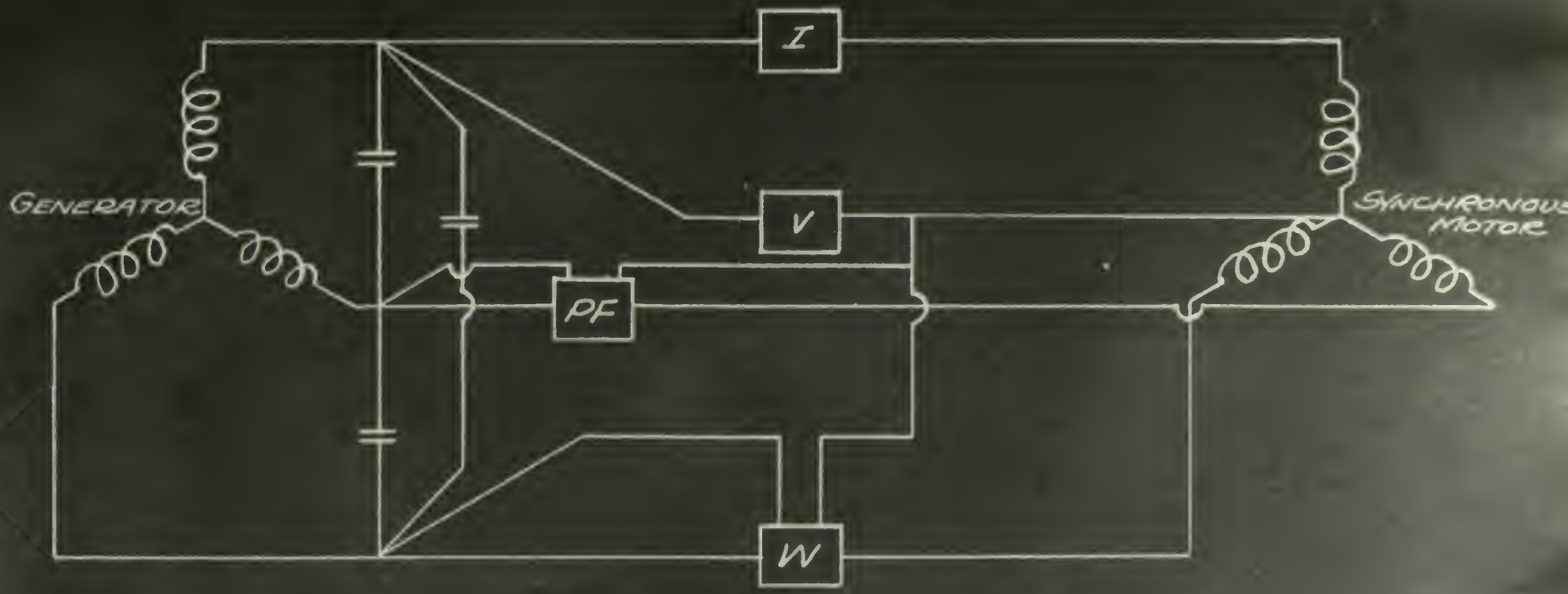

FIGURE 7

EXPERIMENTAL SET-UP FOR THE 0.8 POWER FACTOR RUN WITH THE SHUNT CONNECTED GENERATOR

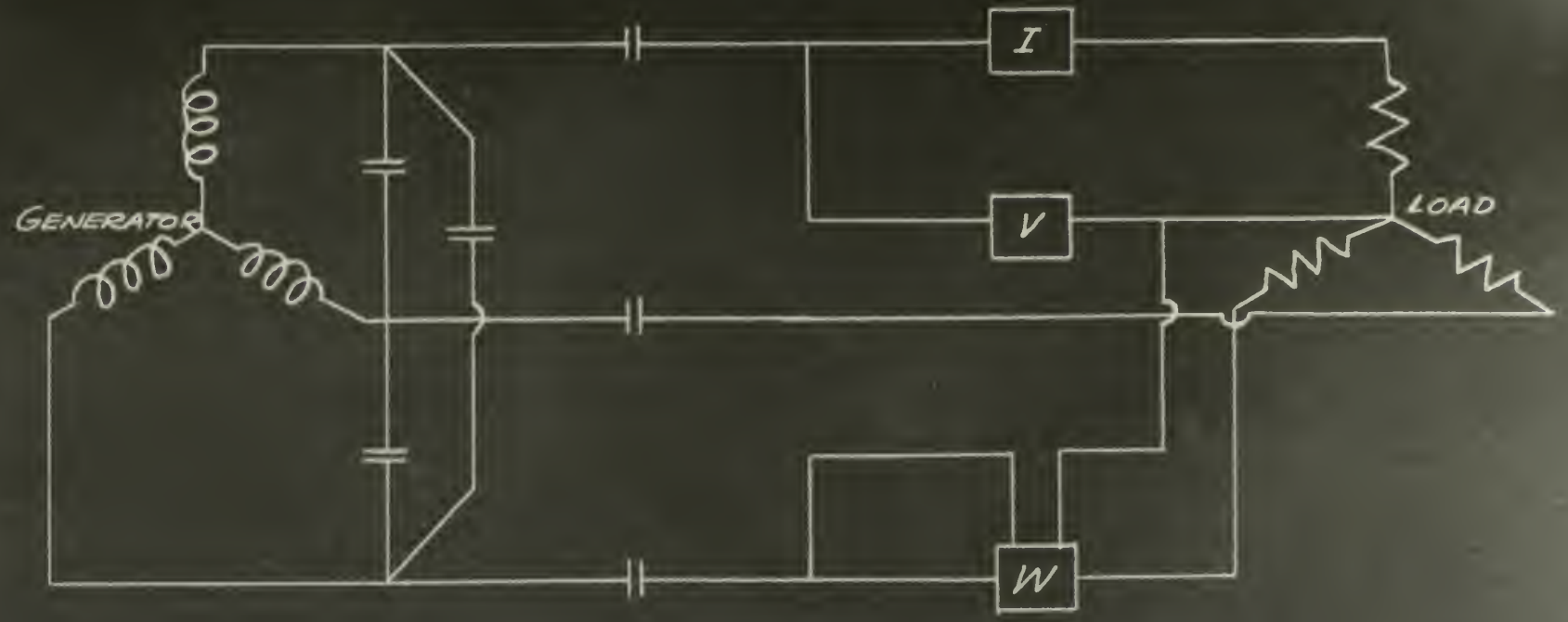

FIGURE 8

EXPERIMENTAL SET-UP FOR THE UNITY POWER FACTOR RUN WITH THE COMPOUNDED GENERATOR

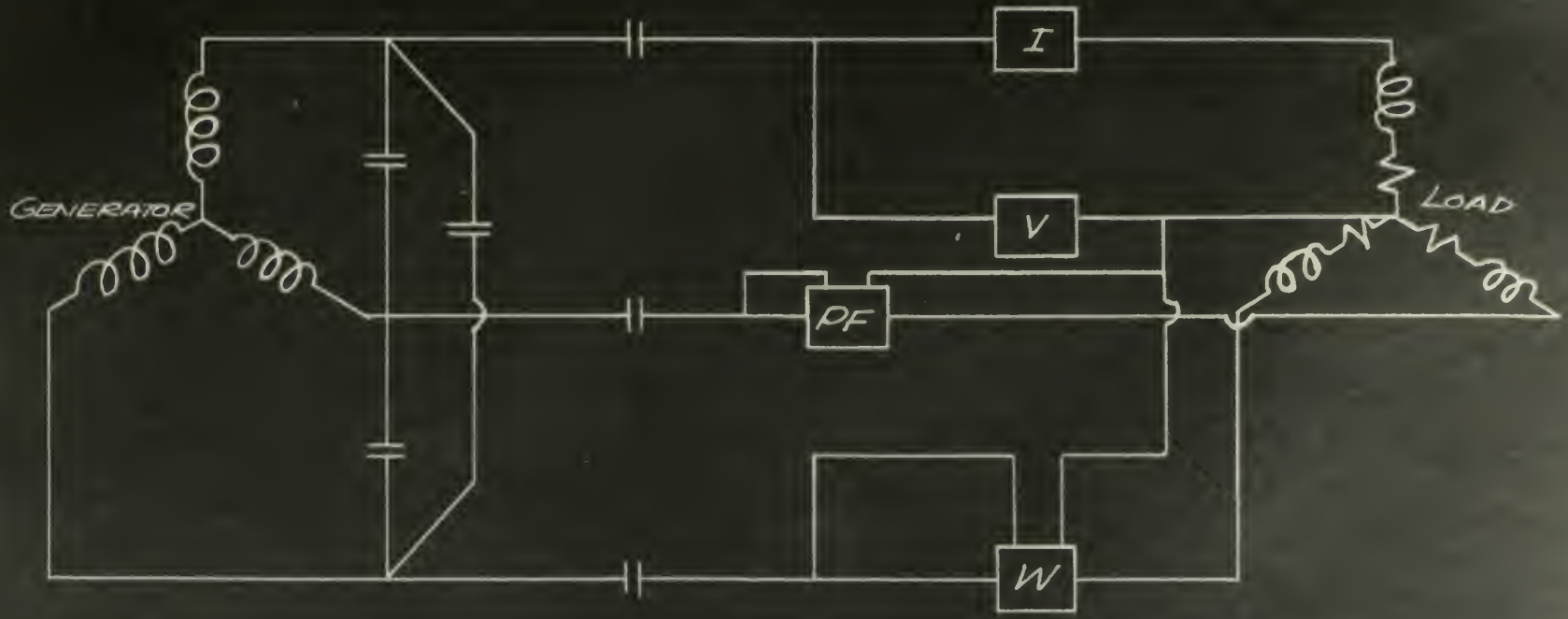

FIGURE 9

EXPERIMENTAL SET-UP FOR THE 0.8 POWER FACTOR RUN WITH THE COMPOUNDED GENERATOR

capacity as possible without exceeding by too much its motor rating. As it was, the current through the generator at no load was about 13 amperes and reached a maximum of about 16 amperes with loading. The motor rating was 13 amperes.

The values of capacitance chosen for the compounded generator were selected to give the performance described in Chapter II, Figure 5, and named an objective in Chapter III.

Chapter V

RESULTS

The results of the unity power factor runs with the shunt connection are shown in Figure 10. The actual results do not agree with the calculated results as closely as desired. The first run was made with the wound resistor bank as a load. When the points determined from the run did not agree with the calculated curve, and no other cause could be found for the discrepancy, it was suspected that the power factor of the load was not unity. Therefore, the power factor of the load was measured with a single-phase, Weston, power factor meter. The power factor meter showed unity power factor as closely as it could be read. No accuracy for the meter was given on the instrument.

However, while the power factor remains practically unity, the tangent of the phase angle changes appreciably. It is the tangent of the phase angle that enters into Equations (4), (5) and (6), which determine the shape of the Y_1 locus. The resistors were not bifilar wound, but were wound in a continous coil, and it was felt that their slight reactance must be responsible for the deviation from the calculated results, though the variation from unity power factor was so slight as to be impossible to measure with the power factor meter, or by the use of voltmeters, ammeters and wattmeters. Therefore, a lamp bank load was used to get a more nearly unity power factor load.

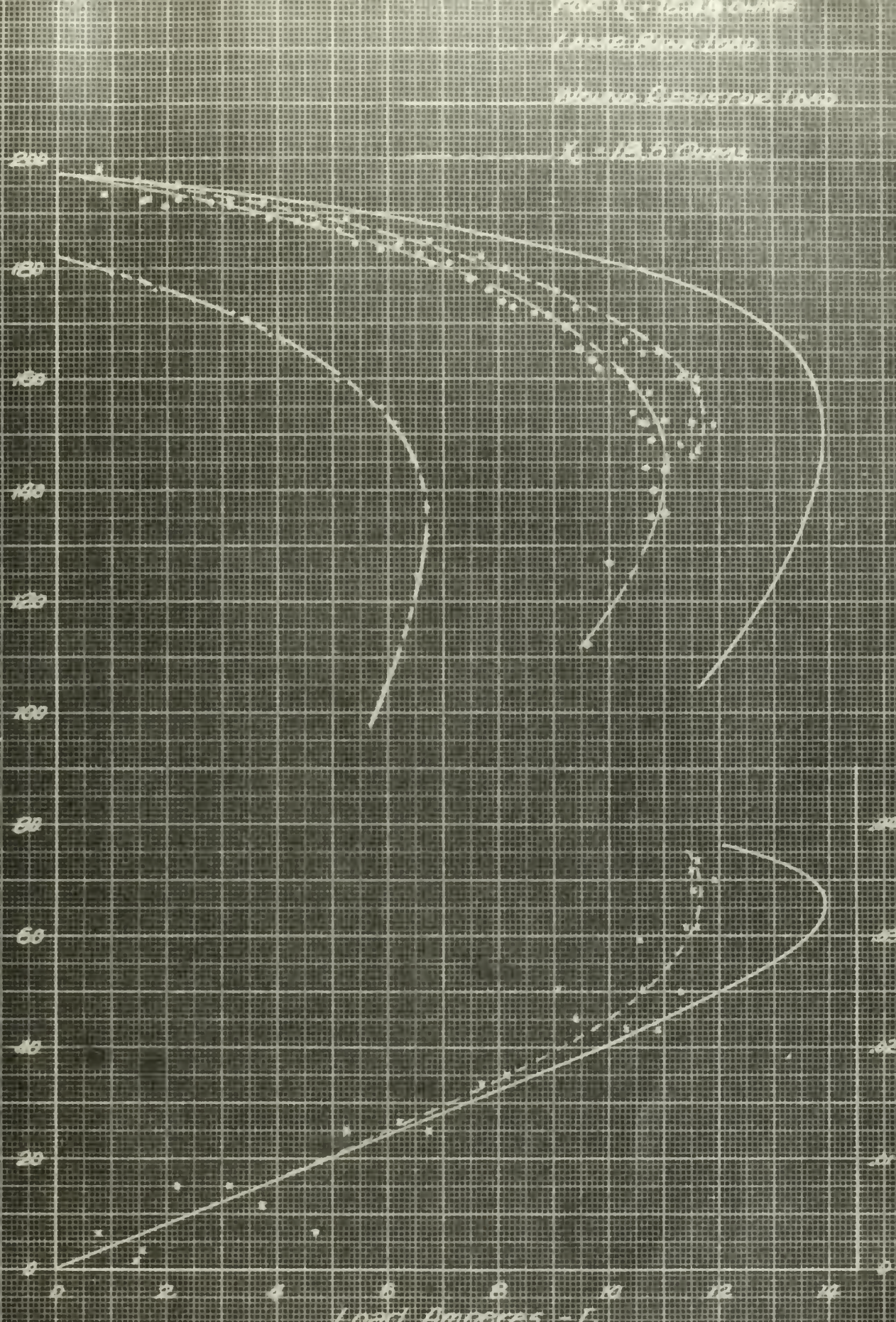

SHUNT CONNECTED GENERATOR - UNITY POWER FACTOR LOAD
EXTERNAL CHARACTERISTIC

FIGURE 10

The lamp bank load did improve the results, as shown by Figure 10. As a matter of interest, the curve for a power factor of 0.998 was calculated and plotted. It was found to coincide with the actual curve for the lamp bank load. The author does not mean to claim or imply that the lamp bank had a power factor of 0.998, but merely to point out that the generator is very sensitive to a lagging power factor, however minute.

One run was made at unity power factor with 143 microfarads per phase for the shunt generator using the resistor bank load. The resulting performance is also shown on Figure 10, in order that it may be easily compared with the runs using 171 microfarads. This demonstrates how rapidly the performance drops off with a decrease in shunt capacitance.

The results of the run at 0.8 power factor for the shunt connection are shown in Figure 11. Experimental points could not be obtained at loads less than 2 amperes, because the synchronous motor required that much current for no-load. It is felt that agreement between the calculated and the experimentally determined curves in this case is quite good.

It is believed that the points at all loads are high, because the slip was too high at each load. The author did not determine the calculated curve until after the run, and so he had no idea what the values of slip should have been for certain loads. The frequency meter was relied on to determine the proper speed. An accuracy of ±2% was claimed

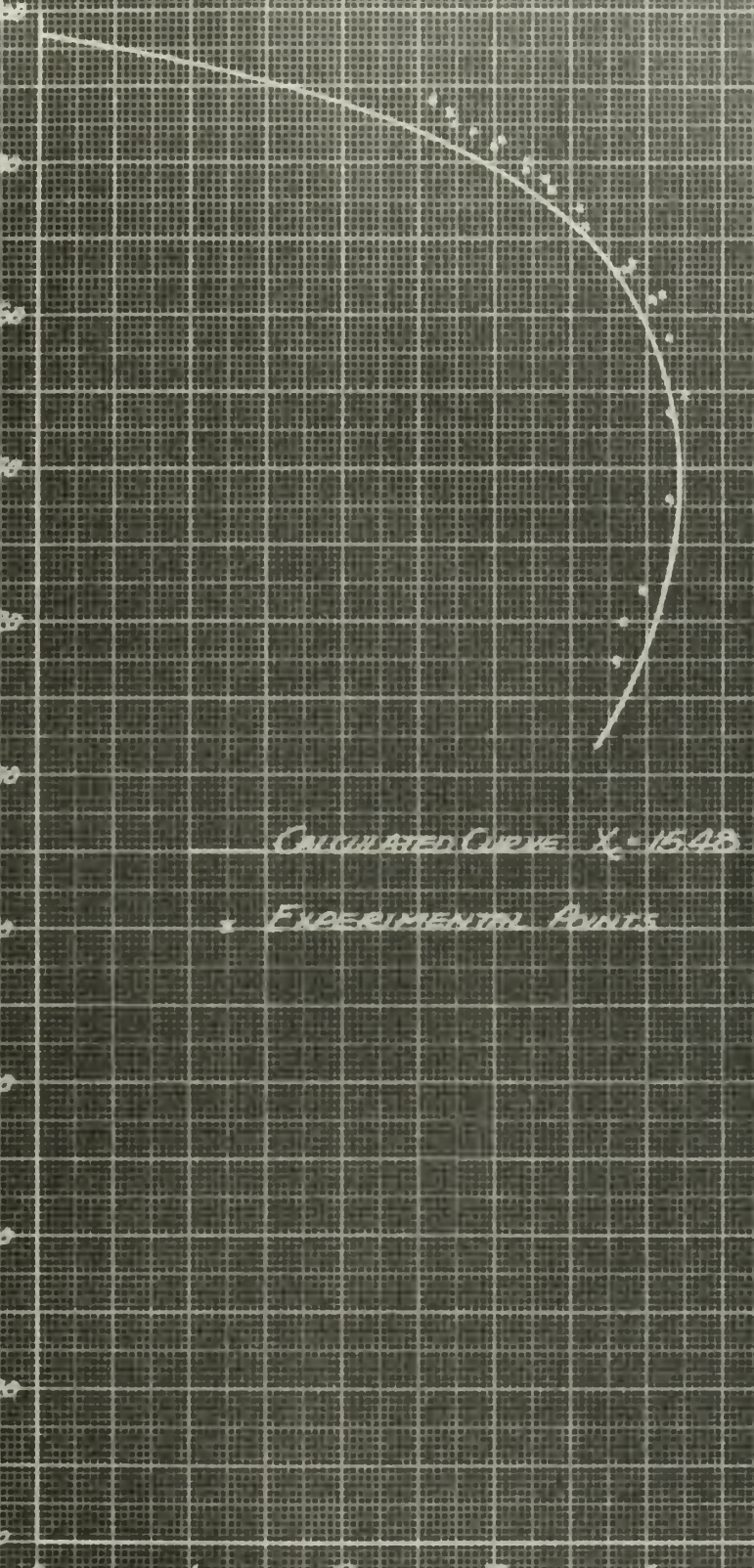

Shunt Connected Generator - 0.8 Power Factor
External Characteristic

FIGURE 11

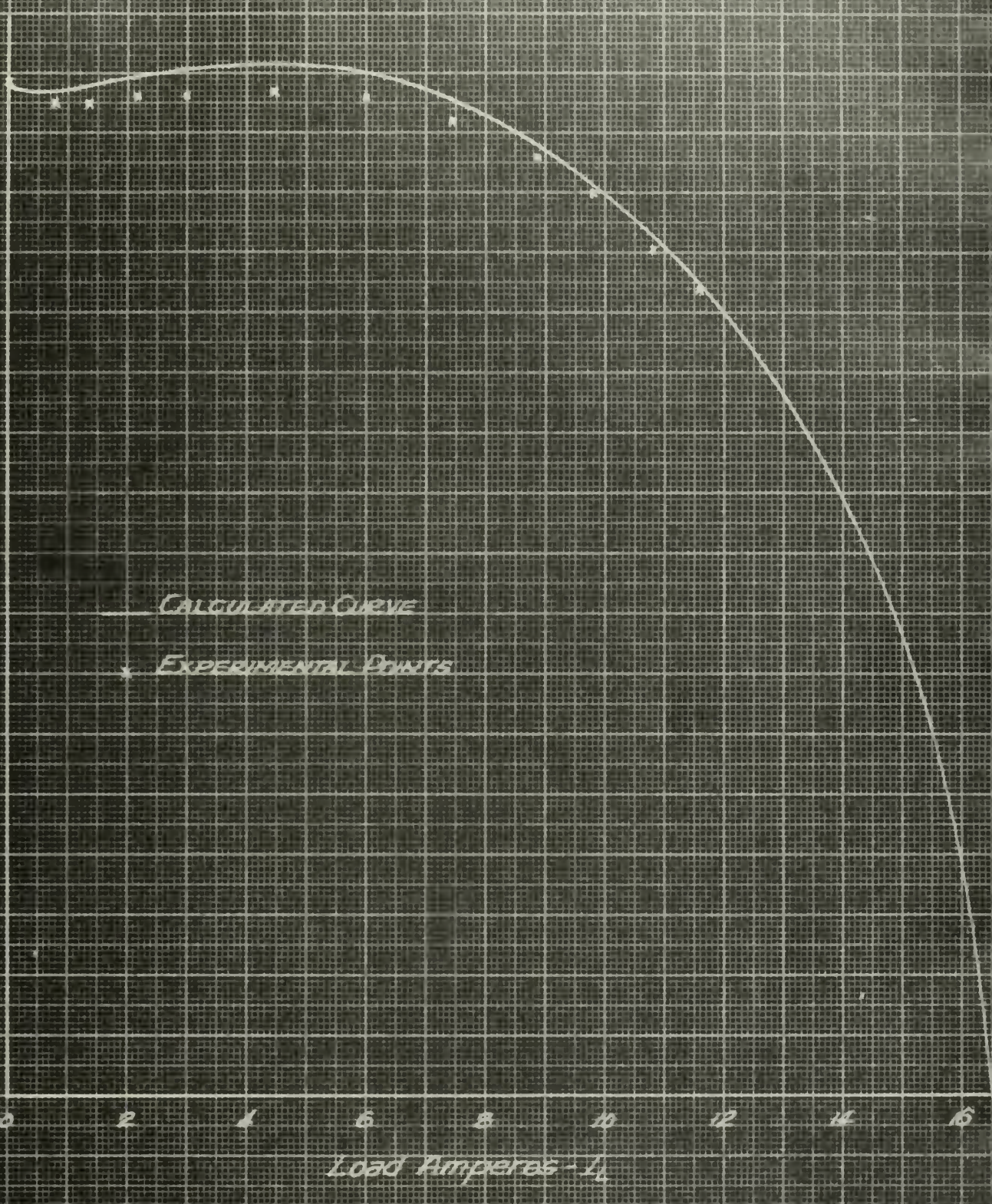

Compound Connected Generator - Unity Power Factor Load

External Characteristic

$X_c = 20.1$ $X_g = 16.0$

COMPOUND CONNECTED GENERATOR - 0.8 POWER FACTOR

EXTERNAL CHARACTERISTIC

$X_c = 20.1$ $X_y = 16.0$

FIGURE 15

for the frequency meter. The slip and points determined are within the accuracy of the frequency meter.

The results of the run with the compounded generator at unity power factor are shown in Figure 12. The lamp bank load was used. Agreement between the calculated and experimentally determined values is considered satisfactory. The deviations of the actual performance from the calculated performance are believed to be caused, in part, by the power factor not being absolutely unity, and by the fact that a great deal of difficulty was experienced in balancing the load at light loads. Small lamps were used to trim the load, and the maximum unbalance in the phase voltages for any reading was 2 volts.

The results of the 0.8 power factor run with the compounded generator are shown in Figure 13. The experimental results in this case were very difficult to determine. The synchronous motor did not offer enough impedance, and tremendous currents, as high as 45 amperes, were drawn from the generator. An induction motor was tried as a load. The full amount of series capacitance shown in Figure 8 was used for starting. The motor would start, but with very little starting torque. The pressure of a loosened prony brake was enough to prevent it from starting. On starting the motor drew about 25 amperes, and as it came up to speed the current rose rapidly to over 40 amperes. To keep the current within reason the series capacitance was reduced by 60

microfarads in each phase as the motor came up to speed. The current through the motor was then about 15 amperes, with about 25 amperes through the generator. As a load was applied to the motor with a prony brake, the current through the motor would decrease. When near 11 amperes the motor would stall, and the current fall to zero. The power factor of the motor was changing from about 0.15 to 0.85 as the load was applied, which considered with the performance characteristics for the compounded generator at lagging power factors, makes such unusual results, if not understandable, at least to be expected.

With the static load made up of the variable inductance in series with the variable resistance it was possible to keep reasonable control of the current and voltage. However, it was extremely tedious to balance the loads and power factors in each leg, the resistance being in steps, rather than continuously variable, and the inductance being varied by pushing laminated iron cores in or out of the inductances.

The experimental points found on the external characteristic curve for 0.8 power factor from no-load to the point where generator action ceases are good. It was possible to balance the voltages to within one or two volts, and to balance the power factors in each leg. Points determined above the point where generator action starts again are not the best that was hoped for. Operation from the point where generator action starts again to the peak voltage was very

unstable. Small changes in the load made such large changes in the voltages that satisfactory balances were impossible to obtain with the equipment and set-up used. The voltage unbalances were about 5 volts for the low voltage readings, and about 15 volts for the last reading. The currents all balanced to within one ampere. The phase voltages and currents were roughly averaged and this average recorded as the reading. An accurate average would have been meaningless. Points were not found beyond the voltage peak, because of overloading the generator.

Chapter VI

CONCLUSIONS

The author feels that the first objective, the verification of Dr. Friauf's method of performance calculation, has been satisfied. For the shunt generator at 0.8 power factor the agreement of the experimentally determined points with the calculated external characteristic curve is good. In view of the demonstrated sensitivity of the generator to lagging power factor loads, especially near the point where excitation is lost and generator action stops, the agreement of the experimental results and the calculated results for the unity power factor runs are considered satisfactory.

The second objective, the verification of the performance characteristics predicted from Figure 5 and shown in Figure 13, was also satisfied. Operation beyond the point where generator action should begin again after having been lost was easily obtained, though not easily controlled.

Operation with the shunt connection is simple and adequate if the load is to remain very near unity power factor. If any load carrying capacity is desired at lagging power factors the shunt connection is not suitable. With the proper choice of series and shunt capacitance, operation with the compound connection near unity power factor can also be satisfactory. If lagging power factor loads are to be carried by the compounded generator some sort of voltage regulation is almost imperative for stable operation.

BIBLIOGRAPHY

1. Bassett, E. D. and Potter, F. M., Capacitance Excitation For Induction Generators, Electrical Engineering, Vol 54: 540-45, 1935.

2. Friauf, J. B., Calculation Of Capacitor Excited Induction Generator Performance, Paper presented at A. I. E. E. Meeting, Providence, R. I., April 26-28, 1950.

3. Langsdorf, A. S., Theory Of A.C. Machinery, McGraw-Hill Book Co. Inc., 1937.

4. Lloyd-Giusti-Chang, Reactance Of Squirrel Cage Induction Motor, A. I. E. E. Transactions, Vol. 66: 1349, 1947.

5. Wagner, C. F., Self Excitation Of Induction Motors, A. I. E. E. Transactions, Vol. 58: 47-51, Feb. 1939.

APPENDIX

1. Susceptance Curve.

The lower portion of the susceptance curve was determined by driving the generator at synchronous speed with the DC motor, varying the impressed primary voltage, and measuring the current. The equivalent circuit for one phase is shown in Figure 15.

The current measured was the magnetizing current, i_m. The voltage drop through the primary impedance, $i_m Z_1$, was subtracted from the terminal voltage, E_T, to give E_m, the voltage across the magnetizing branch of the circuit. The magnetizing current, i_m, divided by the voltage E_m gave the susceptance of the magnetizing branch, b_m. The value of b_m was plotted against E_m to give the susceptance curve.

If the generator could have been driven by a synchronous motor, the curve would have been much more easily and accurately determined, as the slightest variation from the synchronous speed gave a very pronounced change in the terminal voltage. The speed was regulated by setting it roughly with a strobatac, measuring it with the tachometer, and adjusting it accurately to synchronous speed. However, longitudinal shifting of the rotor with the resulting changes in friction drag were enough to cause measurable variations in the current and voltage.

Since three phase voltages above 220 volts were not readily available this portion of the susceptance curve was

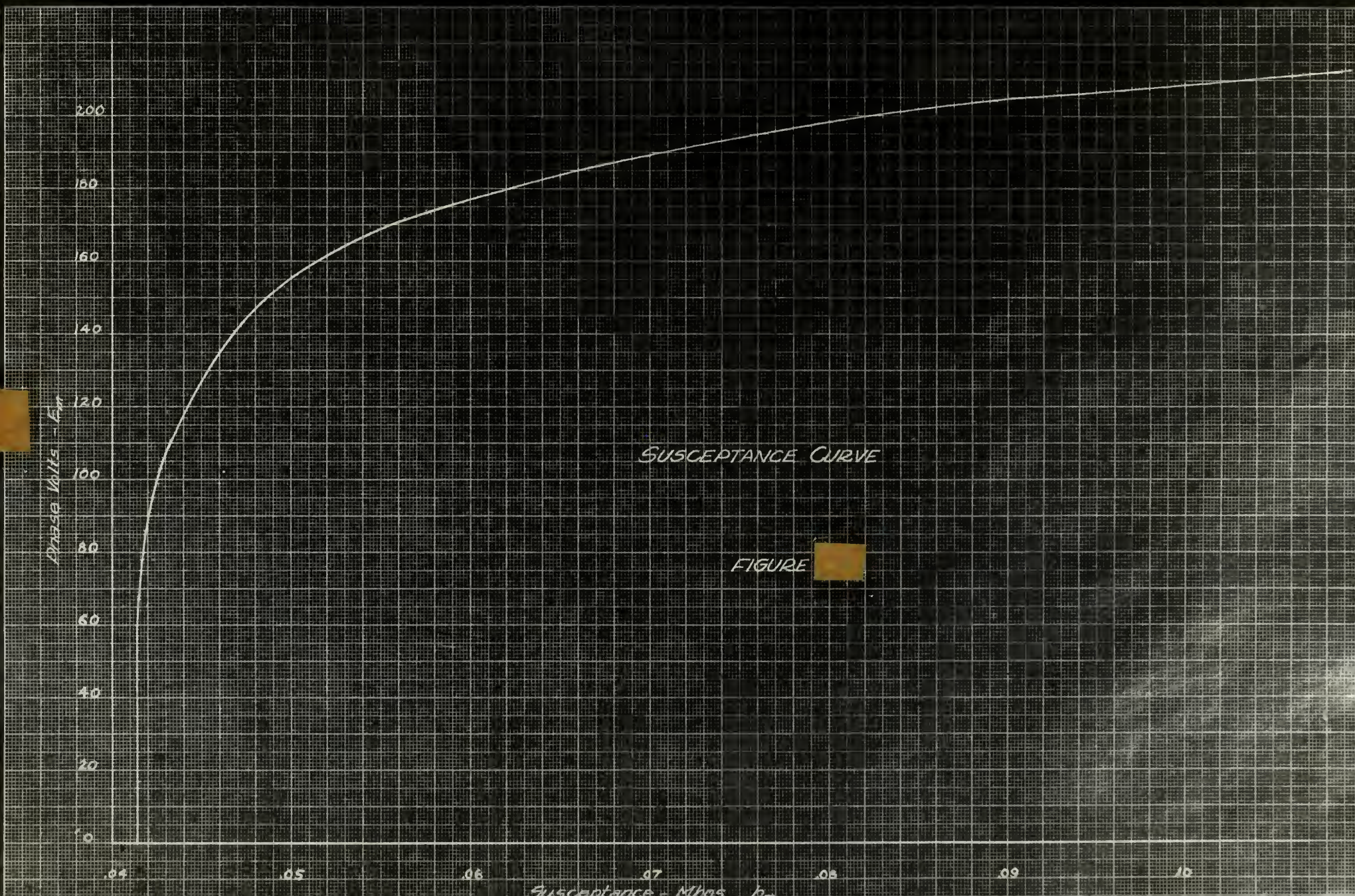

SUSCEPTANCE CURVE

FIGURE

FIGURE 15

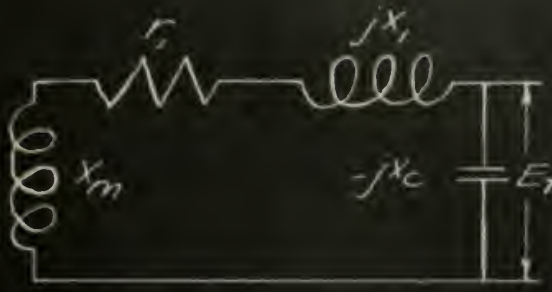

FIGURE 16

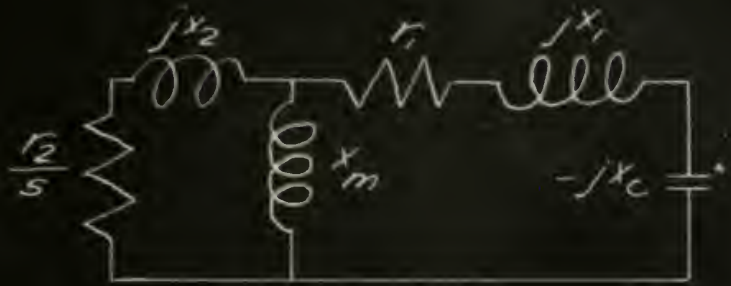

FIGURE 17

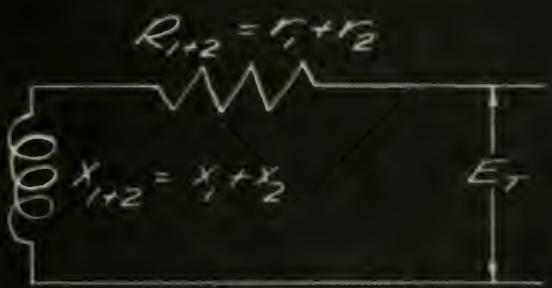

FIGURE 18

OPEN CIRCUIT AND SHORT CIRCUIT
TEST EQUIVALENT CIRCUITS

determined by driving the generator with shunt capacitors for excitation and with no load. By varying the capacitance the no load voltage and exciting current were varied. The equivalent circuit for this system is shown in Figure 16. The more exact equivalent circuit is shown in Figure 17. There will be secondary current. However, this current in the secondary required to produce the magnetizing current at no load is so small that this portion of the circuit may be safely ignored, and the circuit shown in Figure 16 was used.

The speed was regulated in this case to give 60 cycles, and the terminal voltage and the magnetizing current were measured. The susceptance was determined as before.

With capacitor excitation the system was not so extremely sensitive to slight speed changes. Points determined by both methods which overlapped checked well. The susceptance curve determined, and used in the calculations is shown in Figure 14.

2. Blocked Rotor Test.

The blocked rotor test was used to determine the sum of the primary and secondary resistances and reactances. The equivalent circuit for this test is shown in Figure 18.

The rotor was blocked and 110 volts applied to the primary. The phase voltages, currents, and powers were measured. It was necessary to shift the instruments from phase to phase, and to shift instruments when measuring current and power in the same phase. Nine separate runs were made, three for each phase. This is the most important test in determin-

ing the constants of the machine, and as a matter of interest the results are tabulated below.

Volts	Amperes	Watts	Z_{1+2}	R_{1+2}
65.5	41.4	1270	1.582	0.741
66.0	41.5	1330	1.590	0.772
65.9	41.5	1305	1.588	0.758
66.2	42.1	1327	1.572	0.749
66.0	41.4	1340	1.594	0.782
65.5	41.0	1305	1.597	0.776
66.0	41.5	1305	1.590	0.758
66.5	41.4	1350	1.606	0.788
66.3	41.6	1355	1.594	0.783

The resistance and reactance were calculated from the measured values as follows:

$$R_{1+2} = \frac{W}{I^2}$$

$$Z_{1+2} = \frac{E_T}{I}$$

$$X_{1+2} = \sqrt{(Z_{1+2})^2 + (R_{1+2})^2}$$

3. Division of the Total Resistance Between Primary and Secondary.

In order to determine the proper division of the total resistance between the primary and the secondary use was made of the circle diagram. The circle diagram was constructed from the no-load and blocked rotor data, and is shown in Figure 19. Line oo' represents the no-load current. Point B represents the short circuit point. The torque line o'c divides DB such that BC/CD equals R_2/R_1. The torque line

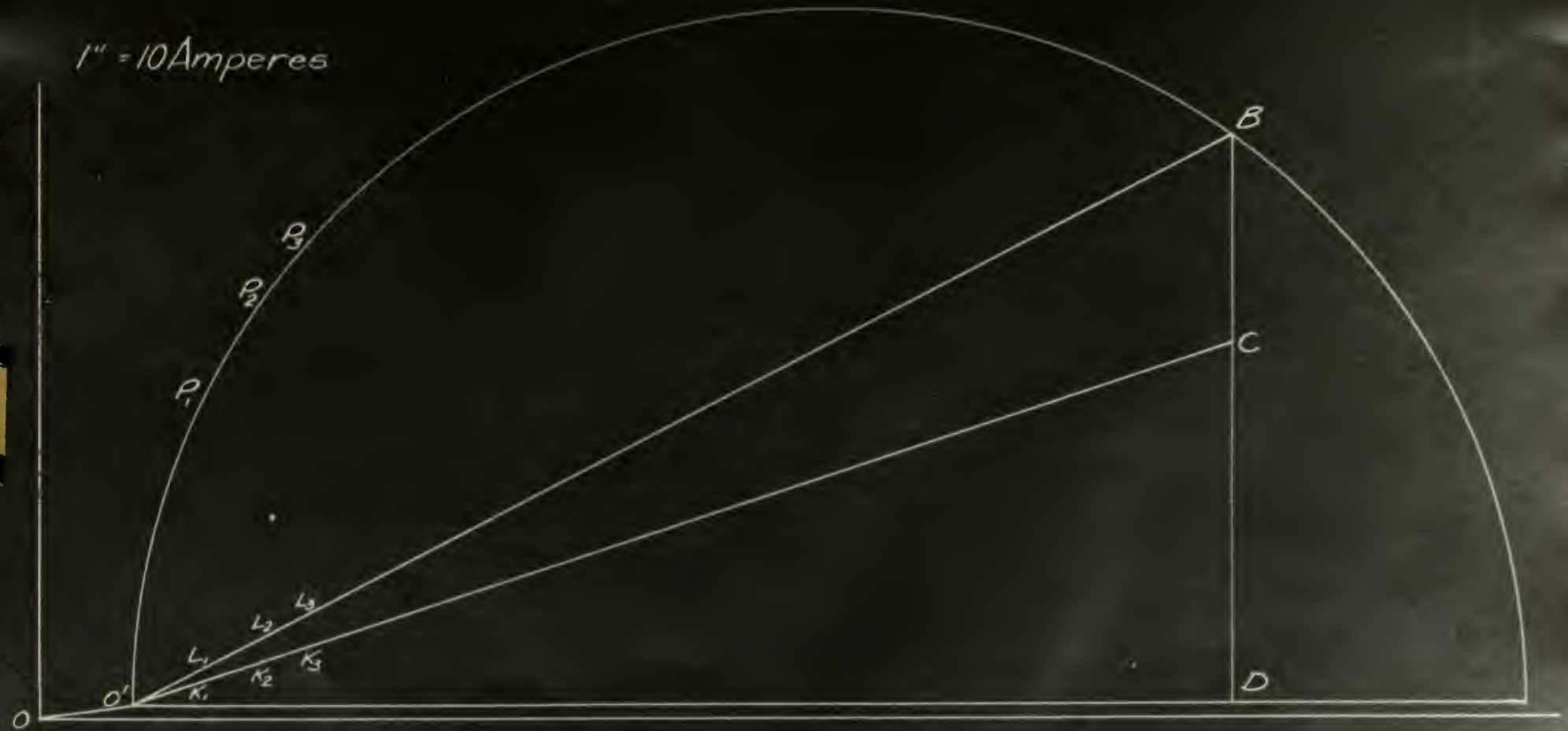

CIRCLE DIAGRAM FOR DETERMINING R_2/R_1

FIGURE

also divides the diagram such that PK/KL equals synchronous speed divided by actual speed.

Three loads were put on the machine by prony brake, and the current and revolutions per minute measured. Points P_1, P_2, and P_3 were thus determined. P_1L_1, P_2L_2, and P_3L_3 were measured on the diagram, and P_1K_1, P_2K_2, and P_3K_3 found from the relation in the preceeding paragraph. These points, K_1, K_2, and K_3, determined the torque line O'C, which was found to divide the line BD such that $R_1 = 0.440$ ohms and $R_2 = 0.253$ ohms.

The DC value of R_1 was measured to be 0.400 ohms by a Kelvin Double Bridge. The value of 0.440 ohms for the effective resistance of the primary was, therefore, very reasonable.

4. Division of the Total Reactance Between Primary and Secondary.

The division of the total reactance between the primary and the secondary was made by calculating the primary reactance from the physical dimensions of the machine. The method of calculation used was that of Arnold as given in a paper by Lloyd-Giusti-Chang[4]. The physical dimensions are given in Figure 20.

The windings were broken into at an end connection and the number of conductors counted. The number of effective conductors was determined by assuming a value for the maximum flux density of 56,000 lines/square inch, and calculating the

number of effective conductors necessary to give a phase voltage of 127 volts. Since the total number of conductors was 14, the number of effective conductors had to be either 1, 2, 7 or 14, the only factors of 14. The calculations gave about 7.5 as the number of effective conductors, so 7 was the obvious choice.

Using the slot dimensions measured and the effective conductors thus determined the value of X_1 was found to be 0.810 ohms.

The division of the primary and secondary reactance is not important. The total reactance is. Arbitrarily dividing the reactance equally between primary and secondary will not make an appreciable difference in the performance found by calculation. The reason for this can be seen on the admittance diagram for the shunt generator. Increasing X_1 and decreasing X_2 gives more curvature to the Y_1 locus, and decreases the curvature of the $-Y_2$ locus, while the difference, Y_m, remains substantially unchanged. This point was investigated by making an equal division and calculating the external characteristic for unity power factor load. The difference was not measurable experimentally.

However, in view of the primary objective of the thesis, and inexperience, the author did not feel justified in making an arbitrary, equal division of the reactance between primary and secondary.

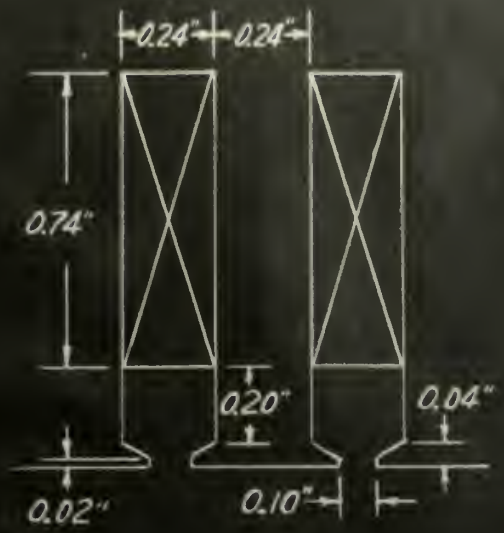

STATOR SLOT

54 Slots

14 Conductors/coil

2 Coil sides/slot

8/9 Pitch

Air Gap 1/32"

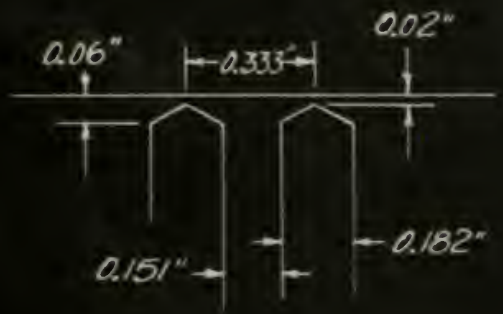

ROTOR SLOT

77 Slots

ROTOR.

FIGURE 20

5. Nameplate Data.

5 KVA

220 Volts

13 Amperes

90% Power Factor

3 Phase

60 Cycles

1200 RPM

Serial Number 4864608

6. Sample Calculations.

See pages 45 and 46.

4-25-50 $r_1 = .447$ $x_1 = .810$ $X_L = 15.98$ 1.0 pf.

$r_2 = .827$ $x_2 = .589$ $-Y_2$ Y_1

S	r_2/s	$(r_2/s)^2$	x_2	x_2^2	$(\frac{r_2}{s})^2 + x_2^2$	g_2	$j b_2$	g_1	$j b_1$	Y_m	E_m	i_1	i_2
0	∞	∞	.589	.391		0	0	0	.06021	.06021	187.0	0	12.77
-.002	163.5	267.332				.0061	.00002	.0061	.06783	.06781	186.5	1.19	12.69
-.004	81.75	668.306				.0122	.00009	.0122	.06790	.06731	186.0	2.27	12.53
-.006	59.5	292.025				.0183	.00020	.0183	.06691	.06671	185.0	3.38	12.39
-.008	40.875	1670.765				.0245	.00035	.0245	.06635	.06600	184.5	4.52	12.22
-.010	32.7	1069.29				.0306	.00055	.0306	.06575	.06520	183.5	5.62	12.05
-.012	27.25	742.563			742.963	.0367	.00079	.0367	.06509	.06430	182.5	6.70	11.88
-.014	23.357	545.599			545.890	.0428	.00107	.0428	.06437	.06330	181.5	7.77	11.68
-.016	20.4375	417.691			418.032	.0489	.00140	.0484	.06360	.06180	180.0	8.80	11.49
-.018	18.1666	330.025			330.366	.0550	.00177	.0550	.06276	.06099	178.0	9.79	11.18
-.020	16.35	267.322			267.663	.0611	.00218	.0611	.06188	.05970	177.0	10.81	10.96
-.022	14.8636	220.927			221.268	.0672	.00264	.0672	.06093	.05829	175.0	11.76	10.67
-.024	13.625	185.640			185.981	.0733	.00314	.0733	.05992	.05678	173.0	12.68	10.38
-.026	12.5769	158.178			158.519	.0793	.00368	.0793	.05887	.05519	170.0	13.48	10.01
-.028	11.6785	136.391			136.728	.0856	.00427	.0856	.05771	.05344	166.0	14.21	9.48
-.030	10.90	118.81			119.15	.0915	.00490	.0915	.05656	.05166	160.0	14.62	9.05
-.032	10.2187	104.423			104.764	.0975	.00557	.0975	.05534	.04977	152.5	14.88	8.44
-.034	9.6764	92.996			92.840	.1036	.00629	.1036	.05409	.04775	144.0	14.90	7.78
-.036	9.08333	82.507			82.848	.1096	.00705	.1096	.05270	.04965	124.0	13.58	6.54
-.038	8.60526	74.050			74.391	.1157	.00785	.1157	.05128	.04343	113.0	13.08	5.79
-.040	8.175	66.831			67.172	.1217	.00869	.1217	.04982	.04113			

Calculations For Unity Power Factor - Shunt Connection

$Z_1 = .490 + j .510$

S	I_1	Z_1	E_{T_j}		$E_{X_j X_{eq}}$		δ_j	
0	-10.33	5.62	197.3	-5.62	.36	12.75	-.36	.02
-.002	-9.75	6.48	196.2	-6.48	.42	12.69	.72	-.05
-.004	-9.16	7.36	195.2	-7.36	.48	12.62	1.79	-.09
-.006	-8.53	8.19	193.5	-8.19	.53	12.50	2.85	-.11
-.008	-7.91	9.04	192.9	-9.04	.58	12.43	3.94	-.21
-.010	-7.29	9.86	190.8	-9.86	.64	12.33	4.98	-.28
-.012	-6.67	10.65	189.2	-10.65	.69	12.22	6.01	-.34
-.014	-6.09	11.43	187.5	-11.43	.79	12.12	7.03	-.44
-.016	-5.40	12.17	185.4	-12.17	.79	11.99	8.01	-.55
-.018	-4.75	12.85	182.7	-12.85	.83	11.81	8.96	-.63
-.020	-4.12	13.58	181.1	-13.58	.88	11.70	9.93	-.74
-.022	-3.47	14.21	178.5	-14.21	.92	11.53	10.84	-.86
-.024	-2.83	14.83	175.8	-14.83	.96	11.36	11.72	-.98
-.026	-2.18	15.34	172.2	-15.35	.99	11.12	12.49	-1.11
-.028	-1.43	15.68	167.9	-15.68	1.01	10.82	13.20	-1.34
-.030	-0.90	15.82	160.9	-15.82	1.02	10.40	13.60	-1.35
-.032	-0.29	15.77	152.8	-15.77	1.02	9.87	13.86	-1.43
-.034	+0.25	15.50	143.7	-15.50	1.00	9.28	13.90	-1.50
-.036	+0.67	13.88	123.3	-13.88	.90	7.97	12.68	-1.43
-.038	+1.06	13.15	111.9	-13.15	.85	7.23	12.23	-1.44

Calculations For Unity Power Factor - Shunt Connection

Thesis 13113
S94 Swift
An investigation of capacitor-excited induction generator performance and a verification of a method of performance calculation.